Journal of Applied Polymer Science

Synthesis and Characterization of a Soybean Oil-Based Macromonomer

David Delatte, Ethem Kaya, Laura G. Kolibal, Sharathkumar K. Mendon, James W. Rawlins, Shelby F. Thames

School of Polymers and High Performance Materials, The University of Southern Mississippi, Hattiesburg, Mississippi 39406
Correspondence to: J. W. Rawlins (E-mail: james.rawlins@usm.edu)

ABSTRACT: An acrylate-functional soybean oil-based macromonomer (SoyAA-1) was synthesized in high yields utilizing sequential amidation and acrylation processes to serve as an internal plasticizer in emulsion polymers. The structure and structure–property relationships of this unique macromonomer were validated with FTIR, NMR, and LC-MS. The viability of SoyAA-1 as a comonomer in emulsion polymerization was established via copolymerization with methyl methacrylate (MMA) at varying copolymer weight compositions. The effect of increasing SoyAA-1 levels and concomitantly higher allylic functionality was measured through film coalescence, minimum film forming temperature, and initial and progressively increasing glass transition temperature(s). The results indicate that synthetic modification of a renewable resource, soybean oil, can yield a valuable monomer that can be copolymerized in high yields via emulsion polymerization to produce practical and mechanically stable latexes for a variety of coatings applications.
 J. Appl. Polym. Sci. **2014**, *131*, 40249.

KEYWORDS: biopolymers and renewable polymers; crosslinking; emulsion polymerization

Received 8 October 2013; accepted 1 December 2013
DOI: 10.1002/app.40249

INTRODUCTION

In recent years, advances in designing and synthesizing environmentally friendly materials have catapulted new developments in the field of polymer chemistry. Furthermore, utilization of renewable resources to develop monomers that can be viable alternatives to petroleum derived raw materials has opened up an innovative market in polymer chemistry. In particular, vegetable oils and their derivatives have been widely utilized to prepare thermoplastics,[1–6] thermoset resins,[7–14] and nanocomposites[15–19] with high biobased content.

Vegetable oils are triglyceride ester of fatty acids that are classified according to their variation in molecular weight, percent unsaturation, conjugation, and functionality. A number of options have been explored for synthesizing vegetable oil-based monomers and polymers. Direct polymerization of the vegetable oils via its allylic functionalities within the fatty acid residue usually yields viscous oils or weak rubbery materials with poor structural integrity.[20] The structural integrity can be improved by copolymerizing vegetable oils with rigid monomers. For instance, cationic copolymerization of vegetable oils with divinylbenzene yielded polymers ranging from soft rubbers to hard plastics.[21] The reactivity of the allylic functionalities within the fatty acid can be increased by introducing polymerizable functional groups.[22] Norbornenyl-functionalized fatty alcohols have been used to synthesize thermosets via ring-opening metathesis polymerization.[23] Synthesis and characterization of vegetable oil-based polyols and their corresponding polyurethanes has been reported by several groups.[24–28] Fatty acid-based monomers have been used to partly replace styrene in vinyl ester resins and reduce styrene emissions.[29] Undecenoic acid, a castor oil derivative, has been utilized to prepare novel polymeric materials via thiol-ene reactions.[30–32]

The soybean crop, Glycine max, is the world's largest source of protein and oil. The US is the world's foremost soybean producer with farmers harvesting 3.056 billion bushels (83.18 million metric tons) of soybeans in 2011.[33] The average MW of soybean oil is 874 and the general fatty acid composition is 7% linolenic acid (C18:3), 51% linoleic acid (C18:2), 23% oleic acid (C18:1), 4% stearic acid (C18), and 10% palmitic acid (C16).[34,35] Soybean oil derivatives have been utilized in many research, product development, and commercialization projects.[36–39] Larock and Lu[40] synthesized a series of methoxylated soybean oil polyols with different hydroxyl functionalities and incorporated them into waterborne polyurethane dispersions. Cadiz and coworkers reviewed developments in biobased polyols and their utilizations in polyurethanes.[41] Soybean oil phosphate ester polyols have been evaluated in low-volatile organic compound (VOC) corrosion resistant coatings.[42] US Pat. No.

7,691,914 describes development of soybean oil-based polyols for use in the manufacturing of polyurethane foams.[43] US Pat. No. 7,799,895 describes a method of low-VOC biobased adhesive compositions utilizing drying oils.[44]

Along similar lines, acrylate functional vegetable oil derivatives have been investigated as comonomers in emulsion polymerization with conventional monomers.[45–49] Fatty acid acrylates such as lauryl acrylate are too hydrophobic for emulsion polymerization.[50] Epoxidized soybean oil acrylate and linseed oil acrylate are highly viscous (25,000 and 100,000 cP at 25°C, respectively) and are employed to impart flow and pigment wetting to ink formulations and in coating formulations to decrease the glass transition temperature (T_g) and increase flexibility.[51] Vegetable oil derivatives with acrylates of the fatty acid backbone exhibit a propensity for chain transfer with the fatty acid double bonds, and the internal acrylates are less reactive than terminal acrylates.[52] Fatty acid acrylates with ethylene glycol as the linking agent between the fatty acid and acrylate moiety result in the hydrophilic ethylene glycol moiety being a part of the final polymer.[53]

Vegetable oil macromonomers (VOMMs) have distinct characteristics that are advantageous in the synthesis of environmentally responsible emulsions: (1) by virtue of its molecular length and large monomer size, the monomers are typically excellent plasticizers and readily facilitate coalescence without the necessity for solvent-based coalescing agents, (2) the monomers readily copolymerize in emulsion polymerization with a variety of vinyl monomers through the acrylate functionality and reduce minimum filming temperature (MFT) during film formation while preserving the allylic functional group (at the polymerization stage), and (3) the allylic functionalities within the fatty acid residue, i.e., monomer tail, react auto-oxidatively after application and slowly during coalescence at ambient temperature, resulting in crosslinked film networks that improve mechanical strength through upward shifted resulting T_gs. The synergistic combination of allylic vegetable oil fatty acids and an acrylic backbone provides mechanically stable, self-crosslinking emulsions with unique structure and design capabilities for utilization in reduced or zero VOC emission coatings.[54–57]

The research reported herein communicates the fundamental development, synthetic methods, and structure–property relationships of a soybean oil macromonomer, Soy AA-1. While one objective is to advance and establish the knowledge of VOMMs, the second is to understand the complexity of retaining the allylic functionality during polymerization and utilizing the same functionality for post-application crosslinking when copolymerized with a commercial monomer, methyl methacrylate (MMA), at varying copolymer compositions.

EXPERIMENTAL

Materials

Chemicals were acquired from several vendors throughout this research project. Soybean oil was purchased from Alnor Oil Company Inc., Valley Stream, NY. *N*-Methyl ethanolamine, 30 wt % sodium methoxide in methanol, acrylic acid, acryloyl chloride, triethylamine (TEA), methoxyhydroquinone (MeHQ), phenothiazine (PTZ), dichloromethane, toluene, isopropanol, sodium bicarbonate, sodium chloride, antimony (III) oxide, ammonium persulfate (APS), MMA, *n*-butyl acrylate (*n*BA), and methacrylic acid (MA), dimethylformamide (DMF), azobisisobutyronitrile (AIBN) were purchased from Sigma-Aldrich, St. Louis, MO. Surfactants Rhodapex® CO-436 and Igepal® CO-887 were obtained from Rhodia, Cranbury, NJ.

VOMM Characterization

Fourier transform infrared spectroscopy (FTIR) was used to monitor monomer synthesis. Aliquots were extracted at regular intervals and applied as thin films onto sodium chloride plates. Spectra were collected for 32 scans on a Digilab FTS 2000 series at a resolution of 4 cm^{-1}. *In situ* FTIR was used to monitor monomer and latex synthesis by collecting spectra with a Si-comp reaction probe at 1 min intervals at a resolution of 4 cm^{-1} on a Mettler-Toledo ReactIR™ 4000. Molecular weight determinations were accomplished via gel permeation chromatography (GPC) using a refractive index (RI) detector and a tetrahydrofuran (THF) mobile phase with toluene as a peak marker. The RI detector was calibrated using polystyrene standards purchased from Polymer Laboratories.

Proton (^{1}H) and carbon (^{13}C) nuclear magnetic resonance (NMR) spectroscopy were performed on a Varian 300 MHz NMR with a relaxation delay of 1 sec to qualify macromonomer structure and quantify the preservation of allylic unsaturation in vegetable oil fatty acids. ^{1}H-NMR spectra were based upon 256 scans and ^{13}C-NMR spectra were based on 1000 scans.

VOMM Copolymer Latex Characterization

Latex particle sizes were determined via the Microtrac® UPA 250 Particle Size Analyzer having a sample range capability of 0.003–6.54 μm (standard deviation ±10 nm) after diluting the latexes with 200 times their volume of deionized (DI) water to a concentration of 2.25×10^{-3} g/mL. The latex MFT was determined visually as the temperature corresponding to the point at which the latex dried to a clear film on the MFFT-BAR instrument (Rhopoint, Inc., temperature range −5 to 90°C). The T_g was analyzed by differential scanning calorimetry (DSC) studies conducted on the DSC Q1000 (TA Instruments) over the temperature range of −90°C to 150°C maintaining a heating rate of 5 °C/min and cooling rate of 10 °C/min for two cycles. Latex films utilized in these studies were coalesced separately under two conditions: (1) nitrogen and (2) air (with 0.1% cobalt drier, metal on latex solids) to understand the plasticizing and film formation functions of VOMM in comparison with the VOMM auto-oxidation with respect to the overall film formation process (chemorheological competition between the processes).

Solid-state NMR spectroscopy was performed on a Varian Unity Inova 400 NMR spectrometer using a standard Chemagnetics 7.5 mm cross polarization with magic angle spinning (CP/MAS) probe. The sample was loaded into a zirconia PENCIL™-style rotor sleeve, sealed with Kel-F™ caps, and spun at rates of 3.5 and 4.0 kHz. Spectra were obtained via direct polarization (DP) using the DEPTH sequence to remove or reduce probe background signals. High-power proton decoupling was implemented during data acquisition to remove C—H dipolar coupling. The acquisition parameters for the DP/MAS spectrum were a recycle delay of 55–70 sec and a ^{13}C 90° pulse width of

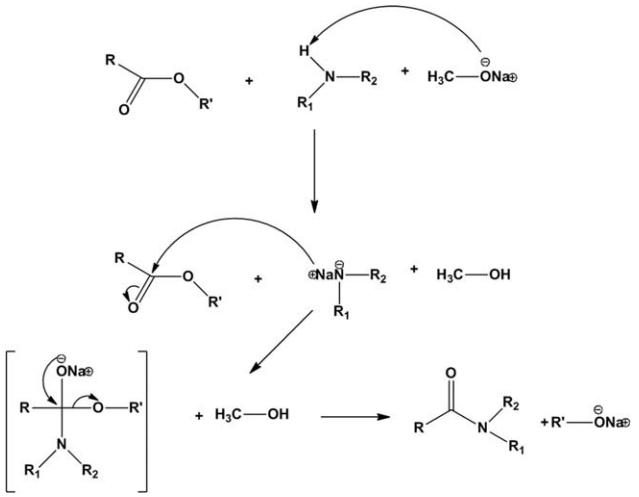

Figure 1. Aminolysis mechanism.[58]

5.5 μsec. The number of scans accumulated was 2,048, and the acquisition time was 45 msec. Exponential line broadening of 10 Hz and zero-filling of 128k was applied to the data prior to Fourier transformation. The baseline was corrected using the Whittaker algorithm as implemented in the MestReNova™ software package.

Soybean Oil Amidation

Soybean oil amide was synthesized via an aminolysis mechanism (Figure 1) following the reaction scheme shown in Figure 2. About 1000 g soybean oil was placed in a 2-L, 3-neck round bottom flask equipped with a heating mantle, nitrogen sparge tube, mechanical stirrer, thermocouple, and condenser. The oil was heated to 100°C and purged with nitrogen for 4 h. Next, the temperature was reduced to 60°C and 393. About 15 g *N*-methyl ethanolamine was added to the flask. The temperature was allowed to equilibrate to 60°C and 15 g of 30% sodium methoxide in methanol was added. At this point, the reaction exhibited an exotherm of 20°C. The reaction progress was monitored via ReactIR to determine overall conversion of the ester to amide functionality by following the peaks at 1763 cm^{-1} and 1640 cm^{-1} respectively. After the ester peak disappeared completely, the reaction was cooled to ambient and the product was transferred to a 4-L separatory funnel for cleanup. About 350 g of dichloromethane was added to prevent solidification during cleanup, washed thrice with 10% brine solution to remove glycerol and residual amine, and dried with magnesium sulfate. The magnesium sulfate was removed via vacuum filtration with a #6 Whatman cellulosic filter paper. Solvents were removed under reduced pressure to yield soyamide (SoyA-1, conversion 99%).

NMR spectral data of SoyA-1 (^{1}H $CDCl_3$): δ 7.26 (imp, $CDCl_3$), 5.35 (m, *4H, —CH=CH—), 3.77 (t, 2H, —N—CH_2—CH_2—OH), 3.55 (t, 2H, —N—CH_2—CH_2—OH), 3.06 (s, 3H, —N—CH_3), 2.96 (s, —N—CH_3), 2.77 (t, 2H, —CH=CH—CH_2—CH=CH—), 2.33 (m,*2H, —N—CO—CH_2—), 2.03 (m, *4H, —CH=CH—CH_2—), 1.63 (m, *2H, —N—CO—CH_2—CH_2—), 1.28 (m, *20H, —CH_2—), 0.97 (t, —CH=CH—CH_2—CH_3), and 0.89 (t, 3H, —CH_2—CH_2—CH_3).

NMR spectral data of SoyA-1 (^{13}C $CDCl_3$): δ 174.6 (—N—CO—CH_2—), 174.1 (—N—CO—CH_2—), 131.76–126.99 (—CH=CH—), 77.20 ($CDCl_3$), 60.72 (—N—CH_2—CH_2—OH), 59.40 (—N—CH_2—CH_2—OH), 52.02 (—N—CH_2—CH_2—OH), 50.86 (—N—CH_2—CH_2—OH), 36.69 (—N—CH_3), 33.57 (—N—CO—CH_2—), 33.50 (—N—CO—CH_2—), 3.07 (—N—CO—CH_2—), 31.83 (×3 —CH_2—), 31.81 (×3 —CH_2—), 31.41 (×3 —CH_2—), 29.66–29.08 (CH=CH—CH_2—, —CH_2—), 27.10 (—CH=CH—CH_2—CH=CH—), 27.08 (—CH=CH—CH_2—CH=CH—), 25.51–24.90 (—N—CO—CH_2—CH_2—), 22.59 (×2 —CH_2—), 22.47 (×2 —CH_2—), 14.18 (×1 —CH_3), 14.02 (×1 —CH_3), and 13.98 (×1 —CH_3).

Soyamide Acrylation

Soyamide was acrylated via two synthetic routes: acryloyl chloride and direct esterification with acrylic acid.[59]

NMR spectral data of SoyAA-1 (^{1}H $CDCl_3$): δ 7.26 (imp, $CDCl_3$), 6.395 (d 2H—C=C—H), 6.06 (t 2H—C=C—H), 5.80(t 2H—C=C—H), 5.35 (m, *4H, —CH=CH—), 4.23 (t,2H, —N—CH_2—CH_2—O), 3.59 (t, 2H, —N—CH_2—CH_2—O), 3.06 (s, 3H, —N—CH_3), 2.96 (s, —N—CH_3), 2.77 (t, 2H, —CH=CH—CH_2—CH=CH—), 2.33 (m,*2H, —N—CO—CH_2—), 2.03 (m, *4H, —CH=CH—CH_2—), 1.63 (m, *2H, —N—CO—CH_2—CH_2—), 1.28 (m, *20H, —CH_2—), 0.97 (t, —CH=CH—CH_2—CH_3), and 0.89 (t, 3H, —CH_2—CH_2—CH_3).

NMR spectral data of SoyAA-1 (^{13}C $CDCl_3$): δ 174.6 (—N—CO—CH_2—), 174.1 (—N—CO—CH_2—), 131.76–126.99 (—CH=CH—), 77.20 ($CDCl_3$), 60.72 (—N—CH_2—CH_2—OH), 59.40 (—N—CH_2—CH_2—OH), 52.02 (—N—CH_2—CH_2—OH), 50.86 (—N—CH_2—CH_2—OH), 36.69 (—N—CH_3), 33.57 (—N—CO—CH_2—), 33.50 (—N—CO—CH_2—), 3.07 (—N—CO—CH_2—), 31.83 (×3 —CH_2—), 31.81 (×3 —CH_2—), 31.41 (×3 —CH_2—), 29.66–29.08 (CH=CH—CH_2—, —CH_2—), 27.10 (—CH=CH—CH_2—CH=CH—), 27.08 (—CH=CH—CH_2—CH=CH—), 25.51–24.90 (—N—CO—CH_2—CH_2—), 22.59 (×2

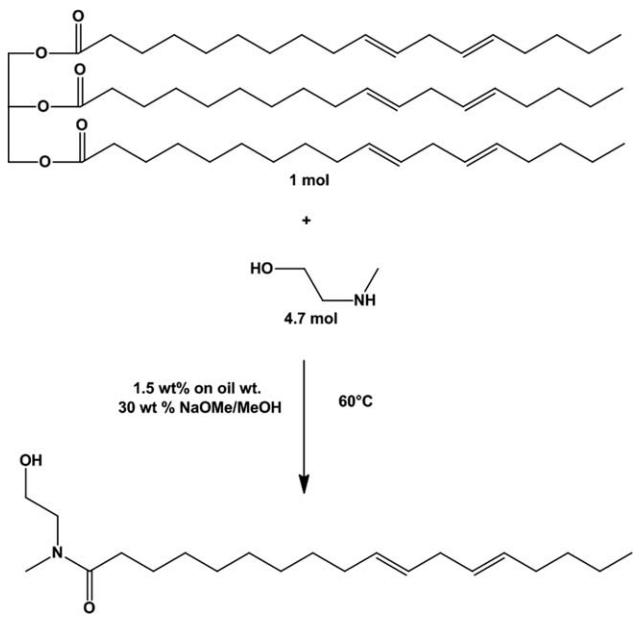

Figure 2. Generalized soybean oil amidation.

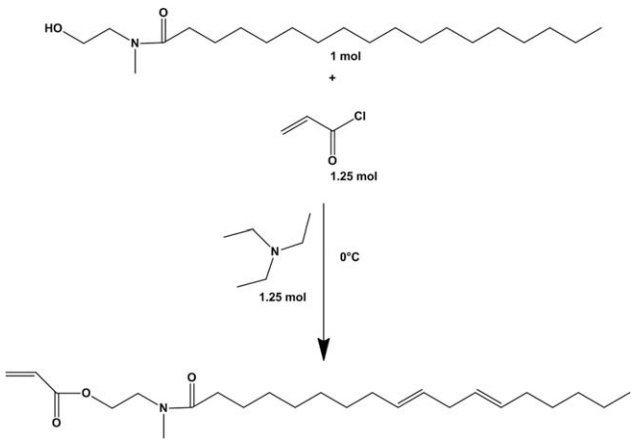

Figure 3. Generalized SoyAA-1 synthesis via acryloyl chloride.

—CH_2—), 22.47 (×2 —CH_2—), 14.18 (×1 —CH_3), 14.02 (×1 —CH_3), and 13.98 (×1 —CH_3).

VOMM Synthesis—Acyl chloride Route

About 200 g SoyA-1, 0.08 g PTZ, 0.08 g MeHQ, 280 g dichloromethane, and 79.14 g TEA were charged into a 1-L 4-neck round bottom flask (Figure 3). Next, 64.35 g of acryloyl chloride and 65 g of dichloromethane were weighed into a 250-mL Erlenmeyer flask, and added to the reactor for 8 h via a peristaltic pump and Tygon® 2075 chemical resistant tubing. The reaction temperature was maintained below 5°C with aid of an ice bath. After complete addition of acryloyl chloride, the reaction was allowed to stand overnight and then decanted into a 1-L separatory funnel. The material was washed thrice with 10% brine solution, followed by 0.2% sodium bicarbonate in brine solution until the pH reached 7. The material was then decanted into a 1-L beaker and magnesium sulfate was added under agitation to remove residual water. The magnesium sulfate was removed by vacuum filtration with a # 6 Whatman filter. Solvents were removed under reduced pressure to yield soyamide acrylate (SoyAA-1, conversion 100%).

VOMM Synthesis—Direct Esterification Route

About 200 g SoyA-1, 85.39 g acrylic acid, 0.43 g PTZ, 0.43 g MEHQ, 1.3 g antimony (III) oxide, and 300 g toluene were charged into a 1-L 4-neck round bottom flask equipped with a thermocouple, heating mantle, nitrogen dispersion tube, mechanical stirrer, Dean-Stark moisture receiver, and condenser (Figure 4). Nitrogen sparge was set to 0.5 L/h. The temperature was raised to 120°C and the reaction continued until the acid value reached a steady minimum. The product was decanted into a 2-L separatory funnel and 60 mL of isopropanol was added to prevent emulsification. The product was then washed with 0.1% sodium bicarbonate in brine solution until the pH reached 7–7.5. The product was decanted into a 2-L beaker and magnesium sulfate was added under agitation to remove residual water. The magnesium sulfate was removed by vacuum filtration with a # 6 Whatman filter. Solvents were removed under reduced pressure to yield soyamide acrylate (conversion ~99%).

VOMM Emulsion Copolymerization

VOMM latexes were synthesized utilizing a starve-fed, semi-continuous polymerization process. The latexes were formulated to a copolymer composition of SoyAA-1/MMA at 10/90, 20/80, 40/60, 60/40, and 80/20 by weight with 0.2 wt % MA at a solid content of 45% by weight. Pre-emulsions were prepared by blending the monomers with DI water, 0.36 wt % Igepal CO-887, 0.54 wt % Rhodapex CO-436, and 0.75% APS. The reaction flask was placed in a water bath at 70°C and purged with nitrogen. The reaction flask was charged with a solution of DI water, 0.11 wt % Rhodapex CO-436, 0.3 wt % sodium bicarbonate, and 0.25 wt % APS, while the contents were stirred continuously at 190 rpm. Five percent of the pre-emulsion was injected into the reaction flask to form seed particles. The reaction continued under starve-fed conditions at a pre-emulsion feed rate of 0.023 mL/sec for 5 h under continuous stirring and nitrogen blanket. Once the pre-emulsion feed was exhausted, the reaction kettle was maintained in the water bath at 70°C for 19 h, then cooled to ambient, filtered, and pH adjusted to 9.0 with ammonium hydroxide.

VOMM Solution Copolymerization

A typical solution copolymerization is (run 4, Table I) discussed here in order to compare and contrast the impact of polymerization process on the multifunctional VOMM. SoyAA-1(20 g, 0.051 mol), MMA (20 g, 0.2 mol), AIBN (0.206 g, 1.26 mmol), and 40 g of DMF were charged to a 100-mL round-bottom flask. Nitrogen was bubbled through the solution for 15 min before the flask was placed in an oil bath at 70°C for 8 h. The polymer was purified by precipitation in methanol and dissolution in THF. After three precipitation cycles, the solid product was dried in a vacuum oven for 16 h at 70°C.

RESULTS AND DISCUSSION

IR Characterization

The amidation reaction was monitored via *in situ* FTIR spectroscopy by following the amide (1640 cm^{-1}) and ester (1763 cm^{-1}) carbonyl peaks (Figures 5 and 6). Multiple SoyA-1 synthesis experiments conducted using the ReactIR 4000 indicated an optimal ratio of 4.5 : 1 amine to oil (by weight) with 1.5 wt % catalyst.

Figure 7 shows the FTIR spectra of soybean oil (a), SoyA-1 (b), and SoyAA-1 (c). Characteristic bands of soybean oil were observed at 3009 cm^{-1} (=CH— stretching of —CH=CH—),

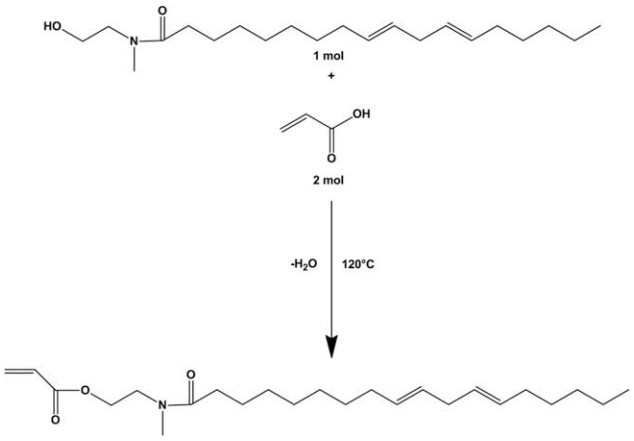

Figure 4. SoyAA-1 synthesis via acrylic acid.

Table I. Solution Copolymerization of SoyAA-1

Run no.	SoyAA-1/MMA[a]	Solvent	Time (h)	AIBN (mol %)	% Unsat.[b]	Yield (%)	M_n (g/mol)	M_w (g/mol)	PDI
1	50/50	bulk	8	0.3	82	44	63,331	122,102	1.93
2	50/50	DMF	8	0.3	87	31	38,142	59,432	1.56
3	50/50	DMF	24	0.3	81	46	45,090	74,756	1.66
4	50/50	DMF	8	0.5	87	39	43,513	68,985	1.59
5	50/50	DMF	8	1.0	84	49	39,831	73,759	1.85
6	50/50	DMF	8	2.0	81	60	44,424	89,765	2.02
7	50/50	DMF	8	4.0	82	85	73,996	248,747	3.36

[a] Feed ratio (wt/wt).
[b] Determined by ^{1}H-NMR.

2926 cm^{-1} (C—H symmetric and asymmetric stretching of —CH_2— and —CH_3), 2855 cm^{-1} (C—H symmetric stretching of —CH_2—), 1746 cm^{-1} (C═O stretching of glyceride ester), 1462 cm^{-1} (—CH_2— scissoring), 1164 cm^{-1} (C—O—C stretching of glyceride ester), and 723 cm^{-1} (—CH_2— rocking).[60] The SoyA-1 spectrum shows new bands at 3399 cm^{-1} (—OH stretching, hydrogen bonding) and 1627 cm^{-1} (C═O stretching of amide). The disappearance of glyceride ester peaks at 1746 and 1164 cm^{-1} and appearance of new peaks validates SoyA-1 formation from soybean oil.

The SoyAA-1 spectra shows a loss of the band at 3399 cm^{-1} (O—H stretching), and the presence of new bands at 1728 cm^{-1} (C═O stretching), 1294 cm^{-1} (C—H stretching), 1269 cm^{-1} (C═O stretching), and 810 cm^{-1} (C—H out-of-plane bending) that confirm the formation of SoyAA-1 from SoyA-1.

NMR Characterization

Figure 8 shows the ^{1}H-NMR spectra of soybean oil, Soy A-1 and SoyAA-1. The soybean oil spectrum shows the glycerol methine proton at 5.27 ppm and glycerol methylene protons at 4.29–4.14 ppm. Lack of these signals in the soyamide spectrum and the appearance of new signals at 3.7 ppm (methylene protons adjacent to the —OH group of —N—CH_2—CH_2—OH), 3.59 ppm (methylene protons adjacent to nitrogen of —N—CH_2—CH_2—OH), and 3.06 ppm (methyl protons of —N—CH_3) verify soyamide synthesis from soybean oil. The shift in the methylene protons adjacent to nitrogen of —N—CH_2—CH_2—OH from 3.7 ppm to 4.3 ppm, shift in the methylene protons adjacent to the —OH group of —N—CH_2—CH_2—OH from 3.59 ppm to 3.66 ppm, and the appearance of the CH_2═CH protons at 5.79 ppm, 6.05 ppm, and 6.33 ppm verifies acrylate synthesis from the amide.

^{13}C-NMR (Figure 9) was utilized to further verify the structures of SoyA-1 and SoyAA-1. Glycerol methine and methylene carbons observed in the soybean oil spectrum at 68.84 and 61.97 ppm, respectively, are no longer observed in the soyamide spectrum; additionally, the carbonyl at 172.9 ppm has shifted to 174.6 ppm. Noting the change from O—C═O to N—C═O, new signals were also noted at 60.72–59.40 ppm (methylene carbon attached to OH of —N—CH_2—CH_2—OH), at 52.02–50.86 ppm (methylene carbon attached to nitrogen of —N—CH_2—CH_2—OH), and at 36.69 ppm (methyl carbon of —N—CH_3). The appearance of new peaks at 165.2 ppm (formation of O—C═O) and the shifting of the peak at 60.72–59.40 ppm (methylene carbon attached to OH of —N—CH_2—CH_2—OH), and at 52.02–50.86 ppm (methylene carbon attached to nitrogen of —N—CH_2—CH_2—OH) further validates the synthesis of SoyAA-1.

LC-MS Characterization

Liquid chromatography-mass spectrometry (LC-MS) was utilized to validate the molecular weight of the intermediate SoyA-1 (Figure 10) and the macromonomer SoyAA-1. The peaks at

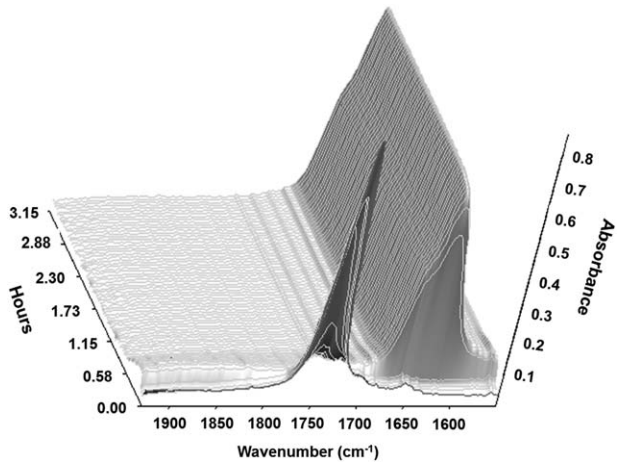

Figure 5. Waterfall plot of SoyA-1 synthesis.

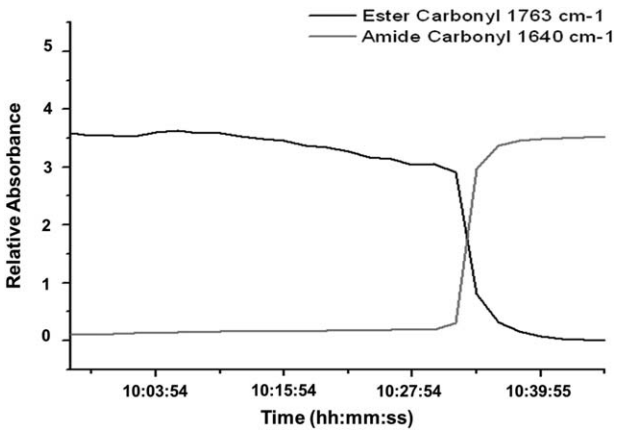

Figure 6. Absorbance to baseline integration for ester and amide peaks.

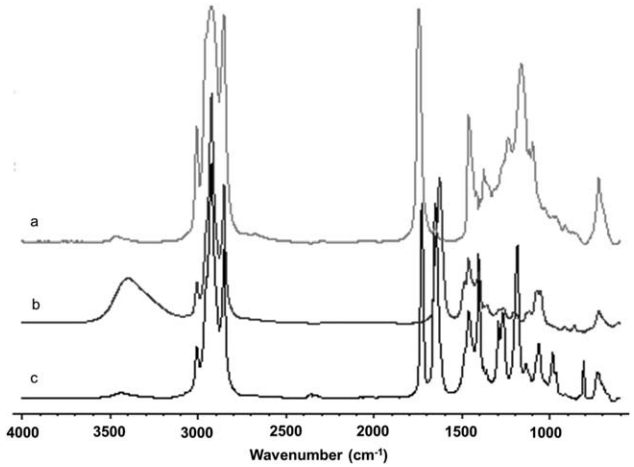

Figure 7. FTIR analysis of soybean oil (a), SoyA-1 (b), and SoyAA-1 (c).

338 g/mol and 392 g/mol validate the formation of SoyA-1 and SoyAA-1, respectively.

VOMM Copolymer Characterization

Latexes with varying levels of SoyAA-1 and MMA were synthesized to elucidate the effect of VOMMs on the glass transition temperature (T_g) and MFT. All latexes were determined to have particles sizes of 140 ± 10 nm. As stated previously, the unsaturated fatty acid functionalities on the VOMM hydrocarbon chain enable VOMM-based latexes to auto-oxidize and create a crosslinked network. The auto-oxidation process was accelerated by the addition of 0.1 wt % cobalt drier (on latex solids). Figure 11 illustrates the T_g changes for 10, 20, 40, 60, and 80 wt % SoyAA-1 latexes between zero cure (films dried in nitrogen) and cure at ambient in six weeks. With increasing VOMM concentration, the overall T_g decreased in both cure states with zero cure temperatures of 88.82°C, 64.16°C, 20.05°C, −15.68°C, and −38.3°C, and final cure temperatures of 93.83°C, 76.39°C, 46.32°C, 13.48°C, and −7.35°C. Consistent monitoring for an additional four weeks confirmed that within the limits of experimental error, polymer self-crosslinking/cure was completed within detectable limits at six weeks of ambient drying/auto-oxidation.

The zero cure data represent a coalescence state where the unsaturated groups of SoyAA-1 have not been exposed to oxygen, thus limiting and/or inhibiting the formation of internal crosslinks. The higher T_g values observed upon ambient cure validate that the fatty acid chains crosslinked auto-oxidatively in the presence of oxygen. The difference between zero and final cure T_g, i.e., ΔT_g, is a measure of the auto-oxidation that has occurred in the latex films and corresponds almost linearly with SoyAA-1 composition (Figure 12). The ΔT_g increase was more profound for latexes containing 40, 60, and 80% VOMM than latexes containing lesser amounts of VOMMs.

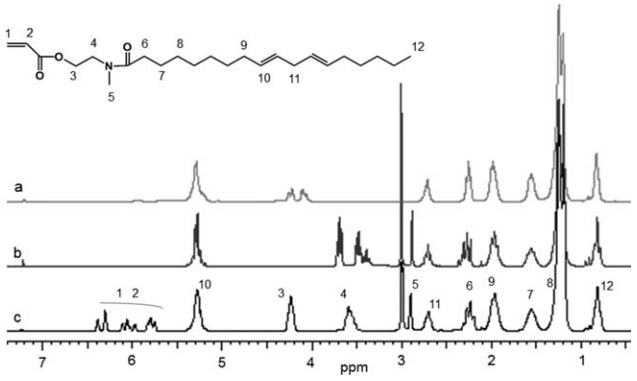

Figure 8. ^{1}H-NMR analysis of soybean oil (a), SoyA-1 (b), and SoyAA-1 (c).

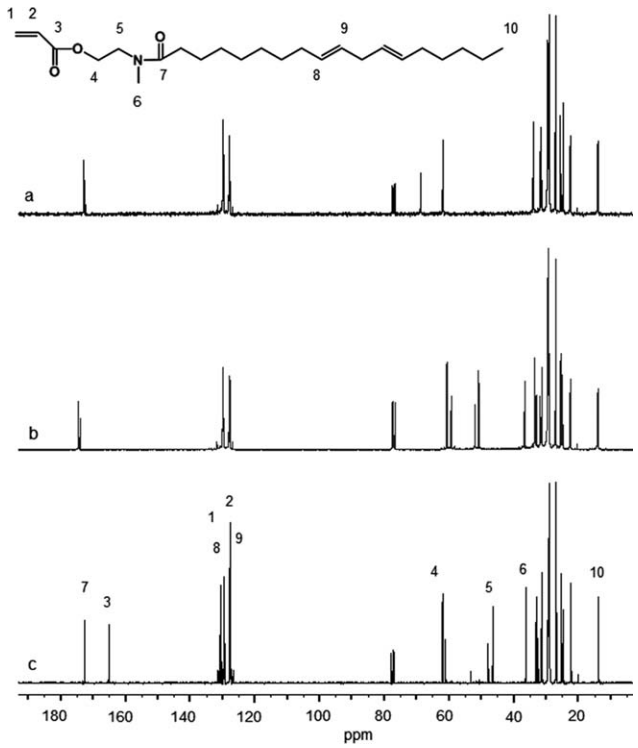

Figure 9. ^{13}C-NMR analysis of soybean oil (a), SoyA-1 (b), and SoyAA-1 (c).

Cure kinetics of SoyAA-1/MMA (40/60 wt/wt) latex films were studied over a 10-week period using percent fatty acid unsaturation values determined via solid-state ^{13}C-NMR. The unsaturation content of the freshly prepared latex indicated that over 96% of the theoretical allylic double bonds were retained during emulsion polymerization. Latex films utilized in this study were dried separately to evaluate auto-oxidation of the VOMM in nitrogen, and in air with and without cobalt drier. Solid-state ^{13}C-NMR spectra of SoyAA-1/MMA (40/60 wt/wt) with 0.1 wt % cobalt drier cured at ambient temperature are illustrated for initial, 1 day, and 7 days dried samples in Figure 13. The peaks appearing between 40 and 55 ppm are attributed to MMA, while the peaks between 125 and 135 ppm are associated with allylic double bonds of SoyAA-1. The ratio of allylic double bonds of SoyAA-1 over MMA was quantified via peak integration to determine the percent unsaturation after polymerization and during auto-oxidative curing.[61–64] It is seen that the peak area of allylic double bonds decreases with time due to auto-oxidative crosslinking catalyzed by cobalt drier. Unlike the samples without drier which retained about 80% of their allylic double bonds even after 10 weeks of drying, samples with cobalt

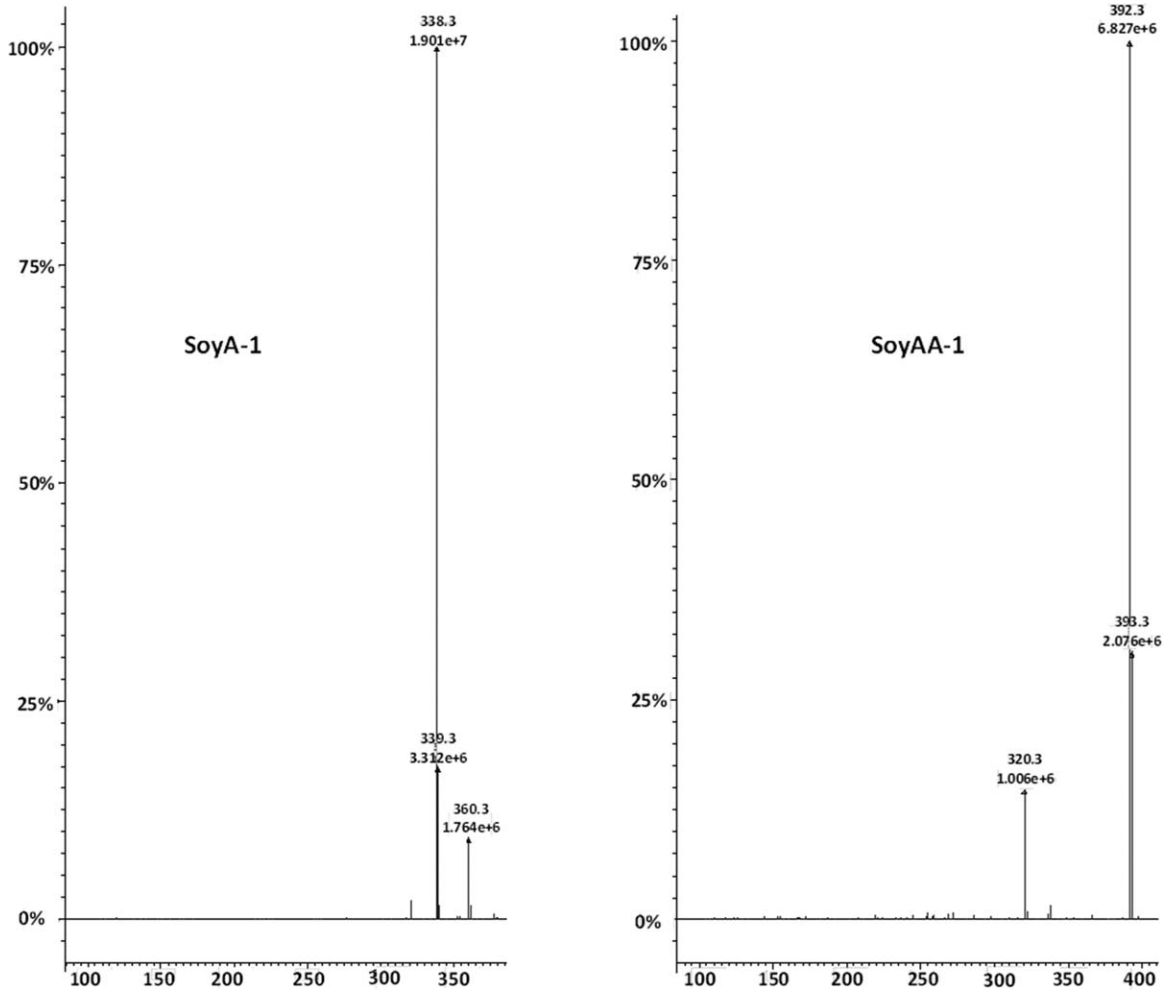

Figure 10. LC/MS analysis of SoyA-1 and SoyAA-1.

drier retained only 10% of their original double bonds at the end of six weeks, and no change was observed after this period.

T_g—MFT Difference

The MFT indicates the temperature at which the forces driving latex deformation exceed the forces that resist deformation.[65] For each latex, MFT depends on a number of factors such as T_g, plasticization by water and cosolvents, and particle size. Sperry et al. suggested that there are two important stages in the process of latex film formation: evaporation of the aqueous solvent and deformation/compaction of particles leading to void closure, and postulated that either of these steps could be rate-

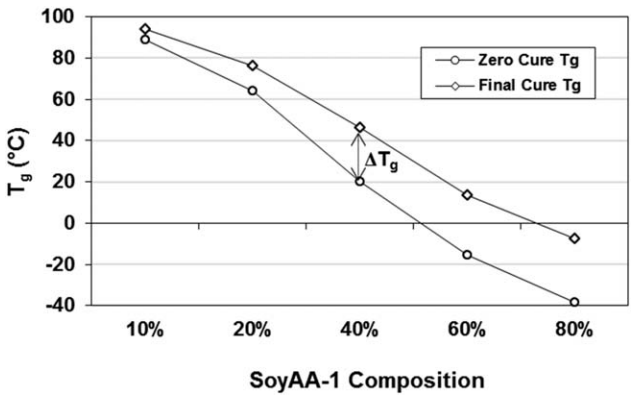

Figure 11. T_g plotted as a function of increasing SoyAA-1 composition at zero and final cure. The ΔT_g is the temperature difference between zero and final cure values.

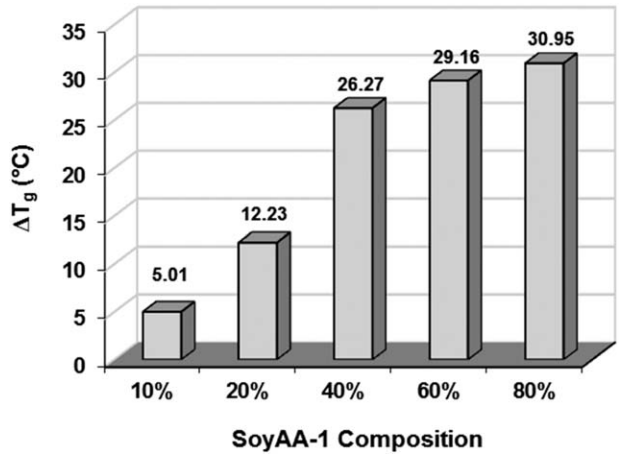

Figure 12. ΔT_g values illustrated as a function of SoyAA-1 composition.

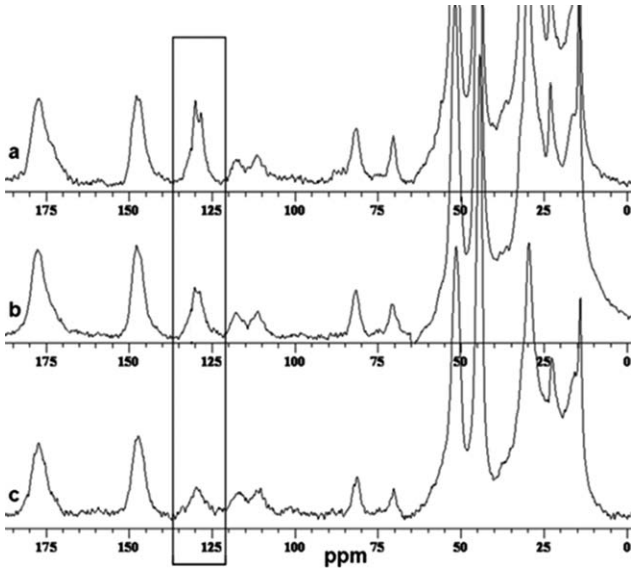

Figure 13. Solid-State ^{13}C-NMR spectra of SoyAA-1/MMA (40/60 wt/wt) with 0.1 wt % cobalt drier cured over (a) initial, (b) 1 day, and (c) 7 days.

limiting, depending on the process temperature.[66] Near its T_g, the rate-limiting step in film formation is particle deformation. When the temperature is more than 20 K above its T_g, evaporation is the dominant rate-limiting process in film formation.[67]

Figure 14 illustrates the MFT-T_g profile of control latexes synthesized via copolymerization of *n*BA and MMA at varying weight ratios. It is clear that the lack of fatty acid unsaturation in the control latexes results in very little difference between the MFT and T_g values.

The MFT-T_g profile of latexes synthesized via copolymerization of SoyAA-1 and MMA is exemplified in Figure 15. It is apparent that increasing SoyAA-1 content has a significant effect on the difference between the MFT and T_g values. Unfortunately, the MFT instrument is incapable of attaining temperatures

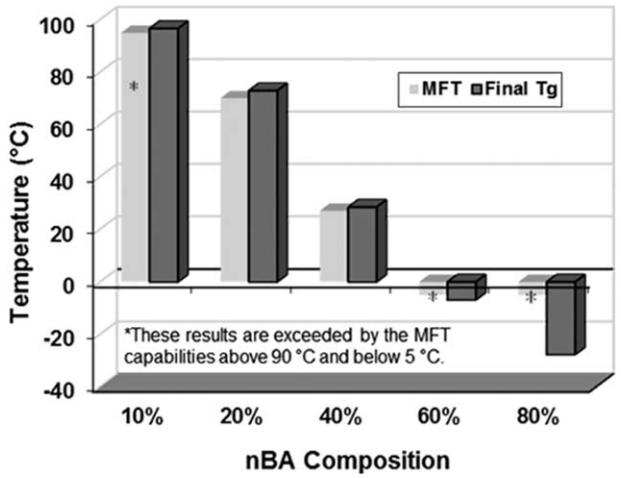

Figure 14. MFFT and final cure T_g values plotted as a function of nBA composition (control latex for comparison with VOMM based-latex results shown below).

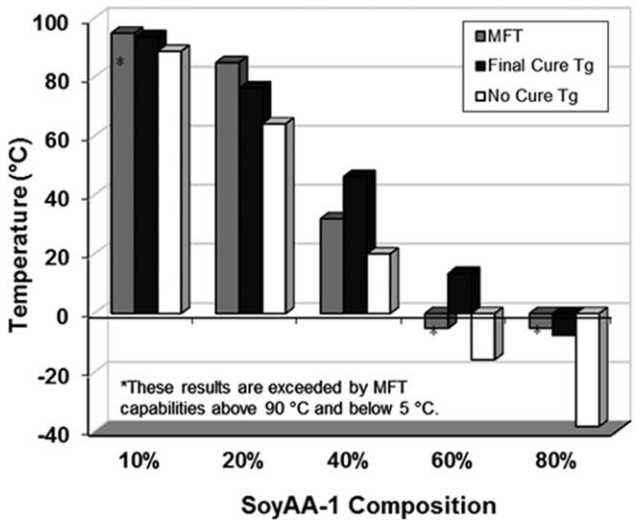

Figure 15. MFT and final cure T_g values are plotted as a function of increasing SoyAA-1 composition.

below −5°C (and thus freezing all samples) and upper temperature of 90°C. Further studies are in progress to elucidate the structure–property relationships of SoyAA-1 latexes and enhance the utility of the MFT-T_g difference that characterizes VOMM latexes.

VOMMs Solution Copolymerization

The copolymerization behavior of VOMMs in solution and bulk was also investigated. SoyAA-1 was copolymerized with MMA at 50/50 by weight via free radical polymerization (Table I and Figure 16). Unlike the copolymers synthesized by emulsion polymerization, all the copolymers described in Table I were soluble in THF.

The data in Table I shows the effect of initiator concentration on percent yield. SoyAA-1/MMA copolymerization conducted in DMF for 8 h with 0.3 mol % initiator resulted in low yield (31%) that was attributed to chain transfer reactions between the VOMMs and growing polymer chains. Increasing the reaction time from 8 h to 24 h raised the yield moderately (46%). Even with 1 mol % AIBN (higher than the initiator amount used in the emulsion polymerizations), the yield was still only around 50%. This indicated that chain transfer was much more pronounced in solution polymerization of VOMMs than with

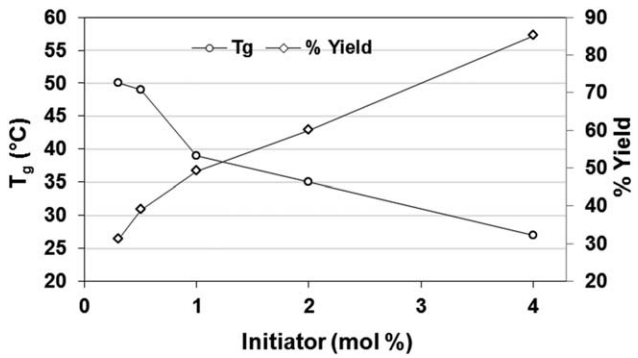

Figure 16. Change in T_g and % yield for solution copolymerization of SoyAA-1/MMA 50/50 (wt/wt) with increasing initiator concentration.

Table II. SoyAA-1 Solution Copolymer T_gs and Compositions

Run no.	T_g (°C)	MMA (mol %)	SoyAA-1 (mol %)	MMA (wt %)	SoyAA-1 (wt %)
1	46	87.1	12.9	63.5	36.5
2	50	88.8	11.2	66.9	33.1
3	47	87.2	12.8	63.6	36.4
4	48	88.3	11.7	65.8	34.2
5	39	86.2	13.8	61.6	38.4
6	35	84.8	15.2	58.8	41.2
7	27	83.8	16.2	57.0	43.0

emulsion polymerization. Black et al. showed that the presence of vegetable oils or vegetable oil derivatives interfered with the copolymerization of MMA and butyl acrylate due to chain transfer reactions and that chain transfer increased at higher concentrations of vegetable oils.[68] Chain transfer in this system resulted from the abstraction of allylic hydrogens by growing polymer chains and reduced the auto-oxidative crosslinking efficiency of the resulting polymers. Increasing the initiator concentration resulted in increase in both the molecular weight and polydispersity index (PDI).

Figure 16 shows that the conversion increases almost linearly with initiator concentration, along with concurrent decrease in the copolymer T_gs. All copolymers (purified as described earlier) were completely amorphous and exhibited a single T_g. Despite the detected impact of chain transfer on the polymerization process, ^{1}H-NMR analysis indicated that the copolymers preserved 81–87% fatty acid unsaturation, an unexpected result.

The ^{1}H-NMR data also provided us the weight and molar composition of the various solution copolymers (Table II). Even though the feed ratio of SoyAA-1/MMA was 50/50 (wt/wt), the copolymer composition was much different, with SoyAA-1 wt % not exceeding 43.0%, indicating that the SoyAA-1 reactivity was lower than MMA in these polymerization conditions.

CONCLUSIONS

The versatile amidation and acrylation process of soybean oil enabled the synthesis of SoyAA-1 in high yields. The macromonomer comprising of both acrylate and allylic functionalities exhibited sufficient hydrophilicity to migrate through the aqueous phase during polymerization, and was successfully incorporated into emulsions via copolymerization with MMA at varying weight ratios. ΔT_g and MFT studies results support successful copolymerization and additionally indicated an almost linear correlation with increasing SoyAA-1 composition and attested to the role of auto-oxidation during the drying of SoyAA-1 latexes for ambient self-crosslinking.

REFERENCES

1. More, A. S.; Maisonneuve, L.; Lebarbé, T.; Gadenne, B.; Alfos, C.; Cramail, H. *Eur. J. Lipid Sci. Technol.* **2013**, *115*, 61.
2. Hojabri, L.; Jose, J.; Leao, A. L.; Bouzidi, L.; Narine, S. S. *Polymer* **2012**, *53*, 3762.
3. Palaskar, D. V.; Boyer, A.; Cloutet, E.; Le Meins, J.-F.; Gadenne, B.; Alfos, C.; Farcet, C.; Cramail, H. *J. Polym. Sci. Part A: Polym. Chem.* **2012**, *50*, 1766.
4. Hazer, D. B.; Hazer, B.; Kaymaz, F. *Biomed. Mater.* **2009**, *4*, 035011.
5. Ilter, S.; Hazer, B.; Borcakli, M.; Atici, O. *Macromol. Chem. Phys.* **2001**, *202*, 2281.
6. Hazer, B.; Demirel, S. I.; Borcakli, M.; Eroglu, M. S.; Cakmak, M.; Erman, B. *Polym. Bull.* **2001**, *46*, 389.
7. Xia, Y.; Quirino, R. L.; Larock, R. C. *J. Renew. Mater.* **2013**, *1*, 3.
8. Moreno, M.; Lligadas, G.; Ronda, J. C.; Galià, M.; Cádiz, V. *J. Polym. Sci. Part A: Polym. Chem.* **2013**, *51*, 1808.
9. Meiorin, C.; Aranguren, M. I.; Mosiewicki, M. A. *Polym. Int.* **2012**, *61*, 735.
10. Stemmelen, M.; Pessel, F.; Lapinte, V.; Caillol, S.; Habas, J. P.; Robin, J. J. *J. Polym. Sci. Part A: Polym. Chem.* **2011**, *49*, 2434.
11. Das, K.; Ray, D.; Banerjee, C.; Bandyopadhyay, N. R.; Mohanty, A. K.; Misra, M. *J. Appl. Polym. Sci.* **2011**, *119*, 2174.
12. Kong, X.; Omonov, T. S.; Curtis, J. M. *Lipid Technol.* **2012**, *24*, 7.
13. Henna, P. H.; Larock, R. C. *Macromol. Mater. Eng.* **2007**, *292*, 1201.
14. Mosiewicki, M. A.; Marcovich, N. E.; Aranguren, M. I. *J. Appl. Polym. Sci.* **2011**, *121*, 2626.
15. Miyagawa, H.; Misra, M.; Drzal, L. T.; Mohanty, A. K. *Polymer* **2005**, *46*, 445.
16. Karak, N.; Konwarh, R.; Voit, B. *Macromol. Mater. Eng.* **2010**, *295*, 159.
17. Konwar, U.; Das, G.; Karak, N. *J. Appl. Polym. Sci.* **2011**, *121*, 1076.
18. Deka, H.; Karak, N. *Polym. Adv. Technol.* **2011**, *22*, 973.
19. Zhu, M.; Bandyopadhyay-Ghosh, S.; Khazabi, M.; Cai, H.; Correa, C.; Sain, M. *J. Appl. Polym. Sci.* **2012**, *124*, 4702.
20. Li, F.; Larock, R. C. *Biomacromolecules* **2003**, *4*, 1018.
21. Li, F.; Hanson, M. V.; Larock, R. C. *Polymer* **2001**, *42*, 1567.
22. Luo, Q.; Lui, M.; Xu, Y.; Ionescu, M.; Petrovic, Z. S. *J. Appl. Polym. Sci.* **2013**, *127*, 432.
23. Xia, Y.; Lu, Y.; Larock, R. C. *Polymer* **2010**, *51*, 53.
24. Xu, Y.; Petrovic, Z.; Das, S.; Wilkes, G. L. *Polymer* **2008**, *49*, 4248.
25. Javni, I.; Petrović, Z. S.; Guo, A.; Fuller, R. *J. Appl. Polym. Sci.* **2000**, *77*, 1723.
26. Husić, S.; Javni, I.; Petrović, Z. S. *Compos. Sci. Technol.* **2005**, *65*, 19.
27. Petrović, Z. S.; Ferguson, J.; Hudson, N.; Javni, I.; Vraneš, M. *Eur. Polym. J.* **1992**, *28*, 637.
28. Kong, X.; Liu, G.; Qi, H.; Curtis, J. M. *Prog. Org. Coat.* **2013**, *76*, 1151.

29. La Scala, J. J.; Sands, J. M.; Orlicki, J. A.; Robinette, E. J.; Palmese, G. R. *Polymer* **2004**, *45*, 7729.
30. van den Berg, O.; Dispinar, T.; Hommez, B.; Du Prez, F. E. *Eur. Polym. J.* **2013**, *49*, 804.
31. Lluch, C.; Ronda, J. C.; Galià, M.; Lligadas, G.; Cádiz, V. *Biomacromolecules* **2010**, *11*, 1646.
32. Lluch, C.; Lligadas, G.; Ronda, J. C.; Galià, M.; Cadiz, V. *Macromol. Rapid Commun.* **2011**, *32*, 1343.
33. The American Soybean Association. Available at: http://www.soystats.com/2012/Default-frames.htm. Last accessed on July 31, 2013.
34. Çakmaklı, B.; Hazer, B.; Tekin, İ. Ö.; Cömert, F. B. *Biomacromolecules* **2005**, *6*, 1750.
35. Li, F.; Larock, R. C. *J. Polym. Sci. Part B: Polym. Phys.* **2000**, *38*, 2721.
36. Larock, R. C.; Lu, Y. *Biomacromolecules* **2007**, *8*, 3108.
37. Mannari, V. M.; Massingill, J. L. *JCT Res.* **2006**, *3*, 151.
38. Boyles, D. A.; Al-Omar, M. S. U.S. Pat. Appl. 0,275,715 (**2009**).
39. Behr, J. M. U.S. Pat. Appl. 0,250,976 (**2008**).
40. Larock, R. C.; Lu, Y. *Biomacromolecules* **2008**, *9*, 3332.
41. Lligadas, G.; Ronda, J. C.; Galià, M.; Cadiz, V. *Biomacromolecules* **2010**, *10*, 2825.
42. Guo, Y.; Mannari, V. M.; Patel, P.; Massingill, J. L. *JCT Res.* **2006**, *3*, 327.
43. Abraham, T. W.; Carter, J. A.; Dounis, D.; Malsam, J. U.S. Pat. 7,691,914 (**2010**).
44. Ddamulari, R. K.; Raidy, J. E.; Wright, B. K. U.S. Pat. 7,799,895 (**2010**).
45. Booth, G.; Delatte, D. E.; Thames, S. F. *Ind. Crops Prod.* **2007**, *25*, 257.
46. Thames, S. F.; Rawlins, J. W.; Mendon, S. K.; Delatte, D. PCT Int. Appl. WO 094,503 A2 (**2008**).
47. Thames, S. F.; Smith, O. W.; Evans, J. M.; Dutta, S.; Chen, L. U.S. Pat. Appl. 0,203,246 A1 (**2005**).
48. Quintero, C.; Mendon, S. K.; Smith, O. W.; Thames, S. F. *Prog. Org. Coat.* **2006**, *57*, 195.
49. Moreno, M.; Goikoetxea, M.; Barandiaran, M. J. *J. Polym. Sci. Part A: Polym. Chem.* **2012**, *50*, 4628.
50. Lau, W. *Macromol. Symp.* **2002**, *182*, 283.
51. Sartomer Company, Inc. Available at: http://www.sartomer.com/newsletter/3062.pdf. Last accessed on July 31, 2013.
52. Diamond, K. L.; Pandey, R. B.; Thames, S. F. *J. Polym. Sci. Part B: Polym. Phys.* **2004**, *42*, 1164.
53. Quintero, C.; Delatte, D.; Diamond, K. L.; Mendon, S. K.; Rawlins, J. W.; Thames, S. F. *Proc. Int. Waterborne High-Solids Powder Coat. Symp.* **2005**, *32*, 348.
54. Thames, S. F.; Rawlins, J. W. *Proc. Int. Waterborne High-Solids Powder Coat. Symp.* **2009**, *36*, 5.
55. Mendon, S. K.; Delatte, D.; Rawlins, J. W.; Thames, S. F. U.S. Pat. Appl. 0,143,527 (**2009**).
56. Kaya, E.; Mendon, S. K.; Rawlins, J. W.; Thames, S. F. *Proc. Int. Waterborne High-Solids Powder Coat. Symp.* **2011**, *38*, 194.
57. Kaya, E.; Mendon, S. K.; Delatte, D.; Rawlins, J. W.; Thames, S. F. *Macromol. Sypm.* **2013**, *324*, 95.
58. March, J. Advanced Organic Chemistry, 3rd ed.; John Wiley & Sons: New York, **1985**; p 375.
59. Furniss, B.; Hannaford, A. J.; Smith, P. W. G.; Tatchell, A. Vogel's Textbook of Practical Organic Chemistry; 5th ed.; John Wiley & Sons: New York, **1989**; p 695.
60. Sharma, B. K.; Adhvaryu, A.; Erhan, S. Z. *J. Agric. Food Chem.* **2006**, *54*, 9866.
61. Alli, A.; Hazer, B. *J. Am. Oil Chem. Soc.* **2011**, *88*, 255.
62. Wutticharoenwong, K.; Soucek, M. D. *Macromol. Mater. Eng.* **2010**, *295*, 1097.
63. Lopes, R. V. V.; Loureiro, N. P. D.; Zamian, J. R.; Fonseca, P. S.; Macedo, J. L.; dos Santos, M. L.; Sales, M. J. A. *Macromol. Sypm.* **2009**, *286*, 89.
64. Cakmakli, B.; Hazer, B.; Tekin, I. O.; Kizgut, S.; Koksal, M.; Menceloglu, Y. *Macromol. Biosci.* **2004**, *4*, 649.
65. Lovell, P. A.; El-Aasser, M. S. Emulsion Polymerization and Emulsion Polymers; Wiley: New York, **1997**; p 489.
66. Sperry, P. R.; Snyder, B. S.; O'Dowd, M. L.; Lesko, P. M. *Langmuir* **1994**, *10*, 2619.
67. Pethrick, R. A.; Cannon, L. A. *Macromolecules* **1999**, *32*, 7617.
68. Black, M.; Messman, J.; Rawlins, J. W. *J. Appl. Polym. Sci.* **2011**, *120*, 1390.